

Performance Evaluation of UAV-Enabled Cellular Networks With Battery-Limited Drones

Yujie Qin, Mustafa A. Kishk¹, *Member, IEEE*, and Mohamed-Slim Alouini², *Fellow, IEEE*

Abstract—Unmanned aerial vehicles (UAVs) can be used as flying base stations (BSs) to offload Macro-BSs in hotspots. However, due to the limited battery on-board, UAVs can typically stay in operation for less than 1.5 hours. Afterward, the UAV has to fly back to a dedicated charging station that recharges/replaces the UAV's battery. In this letter, we study the performance of a UAV-enabled cellular network while capturing the influence of the spatial distribution of the charging stations. In particular, we use tools from stochastic geometry to derive the coverage probability of a UAV-enabled cellular network as a function of the battery size, the density of the charging stations, and the time required for recharging/replacing the battery.

Index Terms—Stochastic geometry, Poisson point process, drone, availability probability, coverage probability.

I. INTRODUCTION

OWING to their freedom of mobility and relocation flexibility, UAVs can be used as flying BSs to provide cellular coverage [1]. In addition, the deployment at relatively high altitudes, compared to terrestrial BSs (TBSs), increases the chances of establishing a line-of-sight (LoS) link with the ground users. This has motivated many works in recent years to study and analyze the performance of UAV-enabled cellular networks [2].

However, the feasibility of UAV-enabled cellular networks still faces many challenges such as limited energy resources, which leads to limited flight time [3]. This, in turn, forces the UAV to interrupt its operation as a flying BS on a regular basis in order to fly back to the charging station to recharge/swap its battery. During charging, the users in the UAV's coverage area need to rely on other resources for cellular services, such as other nearby TBSs [4].

Multiple solutions have been provided in the literature to overcome this issue. Authors in [5] proposed UAV swapping, which suggests having an up and ready UAV to replace the operating UAV as soon as its battery gets drained. Another less expensive solution is battery swapping, which is based on replacing the drained battery with a fully charged one, instead of waiting for the drained battery to be recharged. Authors

in [6] studied the performance of a laser-powered UAV system, where laser beams are used to wirelessly charge the UAV's battery while it is hovering and providing cellular service. Authors in [3], [7], [8] proposed using tethered UAVs, where a trade-off arises between having a stable power supply through the tether and limiting the mobility of the UAV. Authors in [9] proposed an optimal UAV placement approach that maximizes the coverage area while reducing its transmit power. However, given that propulsion power consumption of the UAV dominates the power consumed for wireless communication, solutions that rely on enhancing the communication energy efficiency are not expected to dramatically increase the UAV flight time.

Contributions. This letter studies the influence of the UAV's limited battery, the density of the charging stations, and the recharging/swapping time on the performance of the UAV-enabled cellular network. In particular, we use tools from stochastic geometry to derive the availability probability of the UAV. Next, we use this result to study the impact of the availability probability of the UAV on the coverage probability of the cellular network.

II. SYSTEM MODEL

We consider a UAV-enabled cellular network composed of TBSs and UAVs, where the UAVs are located at the centers of hotspots. In order to model the locations of the users in the hotspot, one of the most popular models in literature is Poisson cluster process (PCP) [10]. There are two possible types of PCP: (i) Thomas cluster process and (ii) Matern cluster process (MCP). In this letter, we model the locations of the users in hotspots using MCP. In particular, the hotspots are modeled as randomly located disks with fixed radius r_c . The centers of the disks, above which the UAVs are deployed, are modeled as a Poisson point process (PPP). Within each disk, the users are uniformly distributed. The UAVs are assumed to hover at a fixed altitude h above each hotspot center. The locations of the TBSs are modeled as a PPP Φ_{TBS} with density λ_t .

Unlike existing literature, the main objective of this letter is to study the impact of the spatial distribution of the charging stations on the performance of the above setup. We model the locations of charging stations as a PPP Φ_c with density λ_c .

A. UAV's Availability

We consider a scenario where each UAV is supposed to fly back to its nearest charging station before running out of energy. During traveling to/from the charging station, as well as during recharging, the UAV is considered unavailable and cannot provide service.

Manuscript received July 1, 2020; revised July 27, 2020; accepted July 28, 2020. Date of publication July 31, 2020; date of current version December 10, 2020. The associate editor coordinating the review of this letter and approving it for publication was G. Geraci. (*Corresponding author: Mustafa A. Kishk.*)

Yujie Qin is with the School of Electronic Science and Engineering, University of Electronic Science and Technology of China (UESTC), Chengdu 610054, China (e-mail: yujie.qin@kaust.edu.sa).

Mustafa A. Kishk and Mohamed-Slim Alouini are with the CEMSE Division, King Abdullah University of Science and Technology (KAUST), Thuwal 23955-6900, Saudi Arabia (e-mail: mustafa.kishk@kaust.edu.sa; slim.alouini@kaust.edu.sa).

Digital Object Identifier 10.1109/LCOMM.2020.3013286

Definition 1 Availability probability: We define the event \mathcal{A} that indicates the availability of the UAV. Conditioned on the distance between the hotspot center and the nearest charging station R_s , the availability probability of the UAV is

$$P_{(\mathcal{A}|R_s)} = \mathbb{P}(\mathcal{A}|R_s) = \frac{T_{se}}{T_{se} + T_{ch} + T_{tra}}, \quad (1)$$

where T_{tra} is the required time to travel to and from the nearest charging station, T_{se} denotes the time spent at the hotspot center to provide cellular service, and T_{ch} presents the total time required for recharging or swapping.

Each of T_{tra} and T_{se} can be formally defined as follows:

$$T_{se} = \frac{B_{\max} - 2P_m \frac{R_s}{V}}{P_s}, \quad T_{tra} = \frac{2R_s}{V}, \quad (2)$$

where B_{\max} is the UAV battery size, P_m denotes the power consumption during traveling, V is the UAV's velocity during traveling, and P_s is the power consumption during hovering at the hotspot center, which includes both the propulsion power and the total communication power. Note that for power consumption during traveling, we focus on the power consumed to travel the horizontal distance R_s since it is typically larger than the power consumed during landing, after reaching the charging station.

Now, the availability probability of the UAV can be derived by taking the expectation of the conditioned probability provided in Definition 1 as follows

$$P_a = \mathbb{E}_{\Phi_c} \left[\frac{T_{se}}{T_{se} + T_{ch} + T_{tra}} \right]. \quad (3)$$

B. Power Consumption

The value of P_s is assumed to be fixed, while P_m is given as follows [11]

$$P_m = P_0 \left(1 + \frac{3V^2}{U_{tip}^2} \right) + \frac{P_1 v_0}{V} + \frac{1}{2} d_0 \rho s A V^3, \quad (4)$$

where U_{tip}^2 is the tip speed of the rotor blade, v_0 is the mean rotor induced velocity in hover, ρ is the air density, A is the rotor disc area, d_0 is fuselage drag ratio, V is the velocity of the UAV, and P_0 and P_1 represent the UAV's blade profile power and induced power in hovering status, respectively. (See (12) and (64) in Ref [11] for more details.) Consequently, the energy consumed during traveling to or from the charging station is

$$E_t = \frac{R_s}{V} P_m = \frac{R_s}{V} \left(P_0 \left(1 + \frac{3V^2}{U_{tip}^2} \right) + \frac{P_1 v_0}{V} + \frac{1}{2} d_0 \rho s A V^3 \right). \quad (5)$$

In the numerical results section, we use the value of V that minimizes E_t , referred to as V_{opt} .

C. User Association

We assume that each user connects to the UAV deployed at its hotspot center if it is available. Otherwise, the user connects to the nearest TBS. Throughout this letter, we focus our analysis on a randomly selected user inside the hotspot, which is referred to as the reference user.

When the user associates with the UAV, the received power is

$$p_u = \begin{cases} p_l = \eta_l \rho_u G_l R_u^{-\alpha_l}, & \text{in case of LoS,} \\ p_n = \eta_n \rho_u G_n R_u^{-\alpha_n}, & \text{in case of NLoS,} \end{cases} \quad (6)$$

where ρ_u is the transmission power of the UAV, R_u is the distance between the reference user and the UAV, α_l and α_n present the path-loss exponent, G_l and G_n are the fading gains that follow gamma distribution with shape and scale parameters $(m_l, \frac{1}{m_l})$ and $(m_n, \frac{1}{m_n})$, η_l and η_n denote the mean additional losses for LoS and NLoS transmissions, respectively.

According to [12], the probability that the UAV has a LoS channel to the reference user is given as

$$P_l(R_u) = \frac{1}{1 + a \exp(-b(\frac{180}{\pi} \arctan(\frac{h}{\sqrt{R_u^2 - h^2}}) - a))}, \quad (7)$$

where a and b are constants that related to the environment and h is the altitude of the UAV. Moreover, the probability of NLoS is $P_n(R_u) = 1 - P_l(R_u)$.

When the UAV is unavailable, the user associates with the nearest TBS. In that case, the received power p_t is given by

$$p_t = \rho_t H R_t^{-\alpha_t}, \quad (8)$$

where ρ_t is the transmission power of the TBS, R_t presents the distance between the reference user and the nearest TBS, and H is the fading gain that follows exponential distribution with average power of unity.

Definition 2 Coverage probability: The total coverage probability conditioned on R_s is defined as

$$P_{cov|R_s} = P_{(\mathcal{A}|R_s)} P_{cov,u} + (1 - P_{(\mathcal{A}|R_s)}) P_{cov,t}, \quad (9)$$

where $P_{(\mathcal{A}|R_s)}$ is given in (1). The unconditioned coverage probability is given by

$$P_{cov} = P_a P_{cov,u} + (1 - P_a) P_{cov,t}, \quad (10)$$

in which,

$$P_{cov,\{u,t\}} = \mathbb{P} \left(\frac{P_{\{u,t\}}}{\sigma^2} \geq \beta \right), \quad (11)$$

where σ^2 is the noise power and β is the signal-to-noise-ratio (SNR) threshold.

III. PERFORMANCE ANALYSIS

In this section, we provide the main results in this letter. We first derive the availability probability conditioned on the distance to the nearest charging station R_s , as well as the unconditioned availability probability. Finally, we use these results to study the coverage probability in the considered system setup.

A. Availability Probability

In this subsection, we analyze the statistics of the availability probability of the UAV. This analysis will be used to study the coverage probability in the next subsection.

Lemma 1 Conditional Availability Probability: Given the value of R_s , the availability probability is given by

$$P_{(a|R_s)} = \frac{B_{\max}V - 2P_m R_s}{B_{\max}V - 2P_m R_s + T_{ch}P_s V + 2R_s P_s}. \quad (12)$$

Proof: The above result follows directly by substituting for (2) in (1). ■

Remark 1: Note that the above expression only holds if $R_s \leq \frac{VB_{\max}}{2P_m}$. Otherwise, $P_{(a|R_s)} = 0$. If this condition is not satisfied, the battery size is not large enough to support energy for the UAV to travel to and from the charging station. Hence, there will not be enough power for the UAV to serve the users in the hotspot. In addition, when $R_s = 0$, the maximum availability probability is achieved. In that case, $P_{(a|R_s=0)} = \frac{B_{\max}}{B_{\max} + P_s T_{ch}}$.

Given that the value of R_s varies from one hotspot to the other, in the below lemma, we derive the CDF of the conditional availability probability.

Lemma 2 CDF of Conditional Availability Probability: The CDF of the conditional availability probability is given by

$$F_{P_{(a|R_s)}}(x) = e^{-\lambda_c \pi C(x)^2}, \quad (13)$$

in which,

$$C(x) = \frac{V(B_{\max}(x-1) + P_s T_{ch} x)}{2(P_m(x-1) - P_s x)}, \quad (14)$$

$$0 \leq x \leq \frac{B_{\max}}{P_s T_{ch} + B_{\max}}. \quad (15)$$

Proof: See Appendix A. ■

In the following theorem, we derive the availability probability.

Theorem 1 Availability Probability: The availability probability of the UAV P_a is

$$P_a = \int_0^{\frac{B_{\max}}{P_s T_{ch} + B_{\max}}} 1 - e^{-\lambda_c \pi C(x)^2} dx. \quad (16)$$

Proof: The above expression follows by substituting the results in Lemma 2 into

$$P_a = \mathbb{E}_{\Phi_c} [P_{(a|R_s)}] = \int_0^{\infty} 1 - F_{P_{(a|R_s)}}(x) dx. \quad (17)$$

B. Coverage Probability

Using the results provided in the previous subsection, we can now study the coverage probability as explained in Definition 2. First, we need to provide expressions for each of $P_{\text{cov,u}}$ and $P_{\text{cov,t}}$, which are provided next.

Lemma 3 Coverage Probability: The coverage probability when associating with a UAV or a TBS are

$$P_{\text{cov,u}} = \sum_{k=0}^{m_1-1} \frac{2}{r_c^2 k!} \int_h^{\sqrt{(h^2+r_c^2)}} P_1(r) r e^{-m_1 g_1(r)} (m_1 g_1(r))^k dr$$

$$+ \sum_{k=0}^{m_n-1} \frac{2}{r_c^2 k!} \int_h^{\sqrt{(h^2+r_c^2)}} P_n(r) r e^{-m_n g_n(r)} (m_n g_n(r))^k dr, \quad (18)$$

$$P_{\text{cov,t}} = \int_0^{\infty} 2\pi r \lambda_t e^{-\pi \lambda_t r^2} e^{-g_m(r)} dr, \quad (19)$$

in which,

$$g_1(r) = \frac{\beta \sigma^2}{\eta_1 r^{-\alpha_1} \rho_u},$$

$$g_n(r) = \frac{\beta \sigma^2}{\eta_n r^{-\alpha_n} \rho_u},$$

$$g_m(r) = \frac{\beta \sigma^2}{r^{-\alpha_t} \rho_t}.$$

Proof: See Appendix B. ■

Due to the direct influence of the availability probability on the coverage probability, and the fact that R_s varies from one cluster to the other, it is important to understand how the value of R_s impacts the coverage probability. In the below lemma, we derive the CDF of the conditional coverage probability described in Definition 2.

Lemma 4 CCDF of Coverage Probability: The complementary cumulative distribution of coverage probability given R_s is

$$F_{P_{\text{cov}|R_s}}(\theta) = 1 - F_{P_{(a|R_s)}}\left(\frac{\theta - P_{\text{cov,t}}}{P_{\text{cov,u}} - P_{\text{cov,t}}}\right), \quad (20)$$

where

$$P_{\text{cov,t}} \leq \theta \leq \frac{B_{\max}(P_{\text{cov,u}} - P_{\text{cov,t}})}{P_s T_{ch} + B_{\max}} + P_{\text{cov,t}}, \quad (21)$$

and $F_{P_{(a|R_s)}}(x)$ is given in (13).

Proof: The above result follows directly by substituting for $P_{\text{cov}|R_s}$ in (13). ■

Remark 2: Note that the range of values of θ in the above result reflects the maximum and minimum achievable values of $P_{\text{cov}|R_s}$. In particular, the minimum achievable value is $P_{\text{cov}|R_s} = P_{\text{cov,t}}$ reflects the scenario where R_s is too large that the UAV is always unavailable. On the other hand, the maximum achievable value is $P_{\text{cov}|R_s} = \frac{B_{\max}(P_{\text{cov,u}} - P_{\text{cov,t}})}{P_s T_{ch} + B_{\max}} + P_{\text{cov,t}}$ reflects the scenario where $R_s = 0$.

IV. NUMERICAL RESULTS

In this section, we compute the value of the coverage probability using the derived analytical results and Monte-Carlo simulations to study the effect of the density of charging stations, the battery size, and the charging time. Unless otherwise specified, the values of the simulation parameters are summarized in Table I.

In Fig. 1, we evaluate the impact of the charging time, the density of the charging stations, and the battery size on the coverage probability. We select a wide range of values for T_{ch} , where low values (such as 5 minutes) represent the scenario of efficient battery swapping while high values (such as 40 minutes) reflect the scenario of slow battery recharging. As can be observed from Fig. 1, the charging time has a significant impact on the value of the density of charging stations required to achieve a specific value of coverage

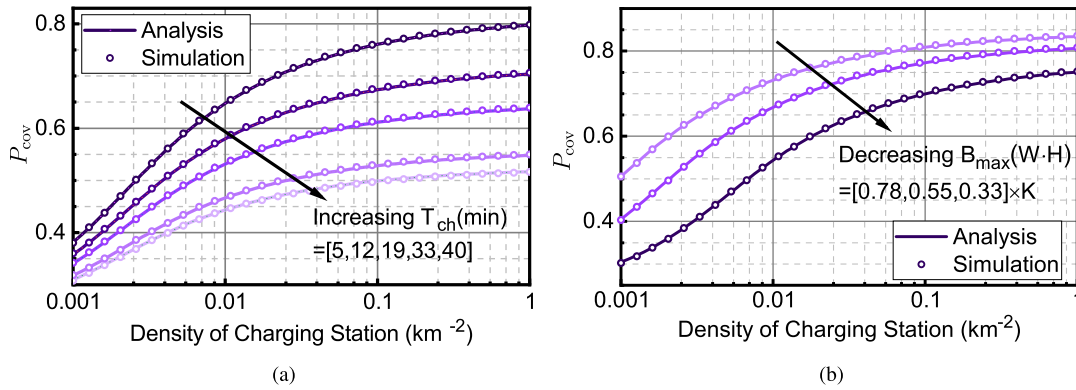


Fig. 1. The variation of the coverage probability with λ_c at (a) different values of T_{ch} , and (b) different values of B_{max} with $K = 177.6$.

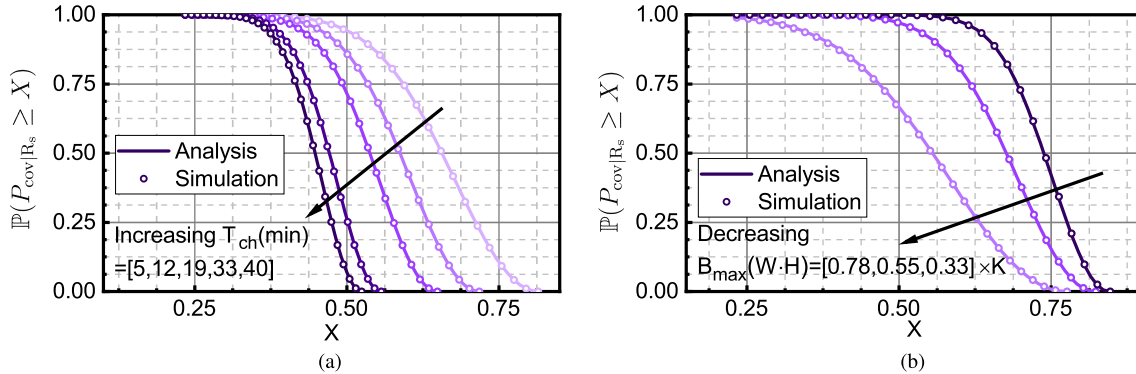


Fig. 2. The CCDF of $P_{cov|R_s}$ at (a) different values of T_{ch} , and (b) different values of B_{max} with $K = 177.6$.

TABLE I
SIMULATION PARAMETERS

Power Consumption [11]			
T_{ch}	5 minutes	B_{max}	88.8 W·H
P_s	177.5 W	λ_c	10^{-2} km ⁻²
V_{opt}	18.46 m/s	P_m	161.8 W
Network Parameters[1]			
ρ_u	0.1 W	ρ_t	10 W
h	60 m	σ^2	10^{-9} W
r_c	100 m	β	20 dB
LoS Parameters		NLoS Parameters	
η_l	0 dB	η_n	20 dB
α_l	2.1	α_n	4
m_l	3	m_n	1
TBS Parameters			
λ_t	10 km ⁻²	α_t	4
Environment Parameters [12]			
a	25.27	b	0.5

probability. For instance, the value of P_{cov} achieved with 1 charging station/km² with charging time of 40 minutes, can be achieved with 100 times less density of charging stations if we can provide more efficient charging stations that have a charging time of 5 minutes. Similar comments also hold for the influence of the battery size B_{max} on the the value of the density of charging stations required to achieve a given value of P_{cov} .

Due to the variation of the coverage probability depending on the value of R_s , we plot in Fig. 2 the CCDF of the coverage probability conditioned on R_s , $P_{cov|R_s}$. This CCDF provides various useful insights about the influence of the charging time and the battery size on the performance. For instance, we observe that the maximum value of the conditional cover-

age probability (which corresponds to the case when R_s goes to zero) decreases from 0.8 to 0.5 as we increase the charging time from 5 to 40 minutes. In addition, we notice that the battery size has higher influence on the minimum value of the conditional coverage probability (which corresponds to the case when R_s goes to infinity).

V. CONCLUSION

In this letter, we derived the coverage probability for a UAV-assisted cellular network as a function of the battery size, the density of the UAV charging stations, and the charging time. Using numerical results, we showed the high impact of the aforementioned system parameters on the system performance. One of the main drawn insights from this letter is the trade-off between deploying high density of low quality charging stations (high charging time) and deploying low density of high quality charging stations (low charging time). Our results showed that we could achieve similar coverage probability with lower density of charging stations if we can reduce the charging time.

APPENDIX

A. Proof of Lemma 2

$$\begin{aligned}
 F_{P_{(a|R_s)}}(x) &= \mathbb{P}(P_{(a|R_s)} \leq x) \\
 &= \mathbb{P}\left(\frac{B_{max}V - 2P_mR_s}{B_{max}V - 2P_mR_s + T_{ch}P_sV + 2R_sP_s} \leq x\right). \quad (22)
 \end{aligned}$$

Given that $P_{(a|R_s)}$ is a decreasing function of R_s , the preimage can be obtained as follows

$$F_{P_{(a|R_s)}}(x) = \mathbb{P}\left(R_s \geq \frac{V(B_{\max}(x-1) + P_s T_{\text{ch}}x)}{2(P_m(x-1) - P_s x)}\right). \quad (23)$$

Given that the minimum value of $R_s = 0$ and its maximum value for a non-zero availability probability is $\frac{B_{\max}V}{2P_m}$ then

$$0 \leq x \leq \frac{B_{\max}}{P_s T_{\text{ch}} + B_{\max}}.$$

B. Proof of Lemma 3

Recalling that $p_l = \eta_l \rho_u G_l R_u^{-\alpha_l}$ and $p_n = \eta_n \rho_u G_n R_u^{-\alpha_n}$, $P_{\text{cov},u}$ in (11) can be rewritten as

$$\begin{aligned} \mathbb{E}_{R_u} \left[\mathbb{P}\left(\frac{p_l}{\sigma^2} \geq \beta | R_u\right) P_l(R_u) + \mathbb{P}\left(\frac{p_n}{\sigma^2} \geq \beta | R_u\right) P_n(R_u) \right] \\ = \mathbb{E}_{R_u} \left[\mathbb{P}\left(\frac{p_l}{\sigma^2} \geq \beta | R_u\right) P_l(R_u) \right] \\ + \mathbb{E}_{R_u} \left[\mathbb{P}\left(\frac{p_n}{\sigma^2} \geq \beta | R_u\right) P_n(R_u) \right]. \end{aligned} \quad (24)$$

Let

$$P_{\text{cov}_l} = \mathbb{E}_{R_u} \left[\mathbb{P}\left(\frac{p_l}{\sigma^2} \geq \beta | R_u\right) P_l(R_u) \right], \quad (25)$$

$$P_{\text{cov}_n} = \mathbb{E}_{R_u} \left[\mathbb{P}\left(\frac{p_n}{\sigma^2} \geq \beta | R_u\right) P_n(R_u) \right]. \quad (26)$$

Then,

$$\begin{aligned} P_{\text{cov}_l} &= \mathbb{E}_{R_u} \left[\mathbb{P}\left(\frac{\eta_l \rho_u G_l R_u^{-\alpha_l}}{\sigma^2} \geq \beta | R_u\right) P_l(R_u) \right] \\ &\stackrel{(a)}{=} \int_h^{\sqrt{h^2+r_c^2}} P_l(r) \mathbb{P}(G_l \geq g_l(r)) \frac{2r}{r_c^2} dr \\ &\stackrel{(b)}{=} \int_h^{\sqrt{h^2+r_c^2}} P_l(r) \frac{\Gamma_u(m_l, m_l g_l(r))}{\Gamma(m_l)} \frac{2r}{r_c^2} dr \\ &\stackrel{(c)}{=} \int_h^{\sqrt{h^2+r_c^2}} P_l(r) \\ &\quad \times e^{-m_l g_l(r)} \sum_{k=0}^{m_l-1} \frac{(m_l g_l(r))^k}{k!} \frac{2r}{r_c^2} dr. \end{aligned} \quad (27)$$

Step (a) is due to the uniform distribution of the users in the disk with radius r_c and $g_l(r) = \frac{\beta \sigma^2}{\eta_l r^{-\alpha_l} \rho_u}$, step (b) follows from the definition: $\bar{F}_G(g) = \frac{\Gamma_u(m, g)}{\Gamma(m)}$, where $\Gamma_u(m, g) = \int_{mg}^{\infty} t^{m-1} e^{-t} dt$ is the upper incomplete Gamma function, and step (c) is from the definition $\frac{\Gamma_u(m, g)}{\Gamma(m)} = \exp(-g) \sum_{k=0}^{m-1} \frac{g^k}{k!}$.

P_{cov_n} can be derived by following similar steps as P_{cov_l} , therefore omitted here.

$$\begin{aligned} P_{\text{cov},t} &= \mathbb{P}(\rho_t H R_t^{-\alpha_t} \geq \beta) \\ &= \int_0^{\infty} \mathbb{P}(H \geq g_m(r)) f_{R_t}(r) dr \\ &= \int_0^{\infty} 2\pi r \lambda_t e^{-\pi \lambda_t r^2} e^{-g_m(r)} dr. \end{aligned} \quad (28)$$

where $f_{R_t}(r) = 2\lambda_t \pi r \exp(-\lambda_t \pi r^2)$ is the contact distance distribution of PPP.

REFERENCES

- [1] B. Galkin, J. Kibilda, and L. A. DaSilva, "A stochastic model for UAV networks positioned above demand hotspots in urban environments," *IEEE Trans. Veh. Technol.*, vol. 68, no. 7, pp. 6985–6996, Jul. 2019.
- [2] M. Mozaffari, W. Saad, M. Bennis, Y.-H. Nam, and M. Debbah, "A tutorial on UAVs for wireless networks: Applications, challenges, and open problems," *IEEE Commun. Surveys Tuts.*, vol. 21, no. 3, pp. 2334–2360, 3rd Quart., 2019.
- [3] M. A. Kishk, A. Bader, and M.-S. Alouini, "On the 3-D placement of airborne base stations using tethered UAVs," *IEEE Trans. Commun.*, to be published.
- [4] M. Alzenad and H. Yanikomeroglu, "Coverage and rate analysis for vertical heterogeneous networks (VHetNets)," *IEEE Trans. Wireless Commun.*, vol. 18, no. 12, pp. 5643–5657, Dec. 2019.
- [5] B. Galkin, J. Kibilda, and L. A. DaSilva, "UAVs as mobile infrastructure: Addressing battery lifetime," *IEEE Commun. Mag.*, vol. 57, no. 6, pp. 132–137, Jun. 2019.
- [6] M.-A. Lahmeri, M. A. Kishk, and M.-S. Alouini, "Stochastic geometry-based analysis of airborne base stations with laser-powered UAVs," *IEEE Commun. Lett.*, vol. 24, no. 1, pp. 173–177, Jan. 2020.
- [7] M. A. Kishk, A. Bader, and M.-S. Alouini, "Capacity and coverage enhancement using long-endurance tethered airborne base stations," 2019, *arXiv:1906.11559*. [Online]. Available: <http://arxiv.org/abs/1906.11559>
- [8] O. M. Bushnaq, M. A. Kishk, A. Çelik, M.-S. Alouini, and T. Y. Al-Naffouri, "Optimal deployment of tethered drones for maximum cellular coverage in user clusters," 2020, *arXiv:2003.00713*. [Online]. Available: <http://arxiv.org/abs/2003.00713>
- [9] M. Alzenad, A. El-Keyi, F. Lagum, and H. Yanikomeroglu, "3-D placement of an unmanned aerial vehicle base station (UAV-BS) for energy-efficient maximal coverage," *IEEE Wireless Commun. Lett.*, vol. 6, no. 4, pp. 434–437, Aug. 2017.
- [10] C. Saha, M. Afshang, and H. S. Dhillon, "Enriched K -tier Het-Net model to enable the analysis of user-centric small cell deployments," *IEEE Trans. Wireless Commun.*, vol. 16, no. 3, pp. 1593–1608, Mar. 2017.
- [11] Y. Zeng, J. Xu, and R. Zhang, "Energy minimization for wireless communication with rotary-wing UAV," *IEEE Trans. Wireless Commun.*, vol. 18, no. 4, pp. 2329–2345, Apr. 2019.
- [12] A. Al-Hourani, S. Kandeepan, and S. Lardner, "Optimal LAP altitude for maximum coverage," *IEEE Wireless Commun. Lett.*, vol. 3, no. 6, pp. 569–572, Dec. 2014.